

Simulation of supersonic flow: comparison of LES against URANS and RANS turbulence models

R. B. Medeiros², J. M. Fusco¹, K. Ropelato², G. Aliatti¹,

¹CENPES – PETROBRAS Research and Development Center, Rio de Janeiro/RJ
(mozartf@petrobras.com.br, aliatti@petrobras.com.br)

²ESSS – Engineering Simulation and Scientific Software Ltda
(rodrigo.medeiros@esss.com.br, ropelato@esss.com.br)

Abstract. *This study aims to analyze the influence of different turbulence models in capturing the flow profile in supersonic nozzles as ones used in steam jet ejectors. Based on the recent experiments by T. Sriveerakul.; S. Aphornratana.; K. Chunnanond [International Journal of Thermal Sciences 46 (2007) 812-822] computations were performed using three different turbulence models, a modified RANS model (SST $k-\omega$), a URANS model with Scale Adaptive Simulation - SAS and the large eddy simulation (LES), with three different steam jet operational conditions, the simulation results were compared with experimental data.*

First, SAS and SST $k-\omega$ computations were performed with three meshes with different refinement level on a mesh independency study. It was observed that SAS model was more sensitive with mesh refinement. In less refined mesh the pressure profile obtained was very close to SST $k-\omega$ results indicating that mesh refinement and time step weren't enough to activate the source term included in ω . With two other meshes a SAS convergence was observed while these meshes are refined enough to use LES.

LES time average values of the variables under study on the most refined mesh were included in the comparison. Furthermore Mach number plots along the equipment center line showed the shock waves formation and the pressure profile recuperation that occurs in the diffuser. The RANS SST $k-\omega$ turbulence model results showed the smallest errors related to the experimental data.

Keywords: CFD, SAS, SST $k-\omega$, LES, supersonic flow and supersonic nozzle.

1 INTRODUCTION

Supersonic nozzles are convergent-divergent nozzle. A pressurized fluid flow through the convergent part, the throat and the divergent portion and then is exhausted in an ambient as a jet. In this process the fluid reaches supersonic velocities.

There are many applications of supersonic nozzles as turbines, dispersers and steam jet ejectors, the latter will be the objective of the present study. These equipments are mechanical components, which allow performing the mixing and/or the recompression of two fluids streams. The fluid with higher total energy is the motive or primary fluid, while the other is the secondary or induced fluid.

During the operation, the motive fluid flows through a convergent-divergent nozzle to reach supersonic velocities while the secondary fluid is drawn and accelerated until shocks, at this point the mixing between the fluids occurs (MAN, 1997).

The literature present several CFD studies concerned on to simulate ejector's flows. SCOTT *et al.* (2008) simulate an ejector used in refrigeration system, comparing numerical results with experimental data, achieving good results with a maximum of 10.8% of error. SRIVEERAKUL *et al.* (2006) has set up an experimental apparatus for an ejector working with saturated water vapor, measuring the wall pressure profile along the ejector and the entrainment ratio (rate between secondary mass flow and primary mass flow), comparing with numerical results obtained in CFD simulations.

Both work previously cited realized steady state simulations using a RANS (Reynolds Averaged Navier-Stokes) model k- ϵ to model the turbulence. In the present work, a CFD package (FLUENT) was used to obtain results of simulations using RANS, URANS and LES approaches for turbulence based on the equipment and data of SRIVEERAKUL *et al.* (2006).

2 METHODOLOGY

The effects of operating conditions and geometries on its performance were investigated and validated with the actual values. In this work were performed 3D simulations of a steam ejector with dimensions showed in Figure 1, based on SRIVEERAKUL *et al.* (2006) geometry.

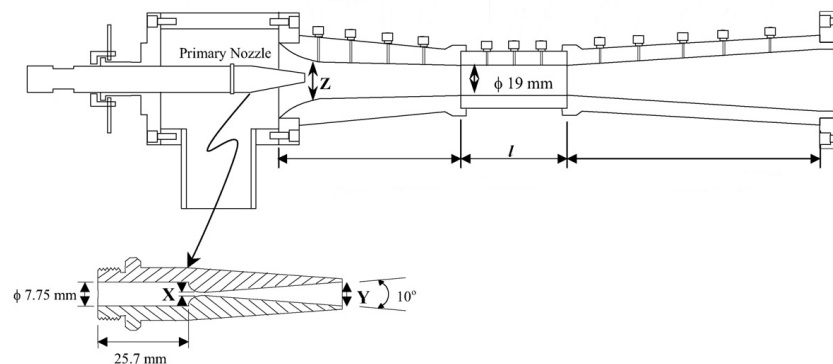


Figure 1: Steam Ejector Dimensions (SRIVEERAKUL *et al.*, 2006).

Saturated water vapor was used as work fluid for primary and secondary fluid in different conditions as showed in Table 1.

Table 1: Saturated water vapor conditions for simulation.

	Primary Fluid		Secondary Fluid	
	Temperature (°C)	Pressure (Pa)	Temperature(°C)	Pressure (Pa)
Case 1	120	198.540	10	1.227
Case 2	130	270.130	5	872
Case 3	130	270.130	10	1.227

In these three cases was assumed the pressure of 3000 Pa as the back pressure and a pressure profile was obtained along the steam ejector wall to compare with experimental data.

An important parameter for the ejector performance evaluation is the entrainment ratio (RM) defined by the equation below.

$$RM = \frac{\text{Secondary Mass Flow}}{\text{Primary Mass Flow}} \quad (1)$$

Consider a typical performance curve of a steam ejector for the specified primary and secondary flow pressures as shown in Figure 2.

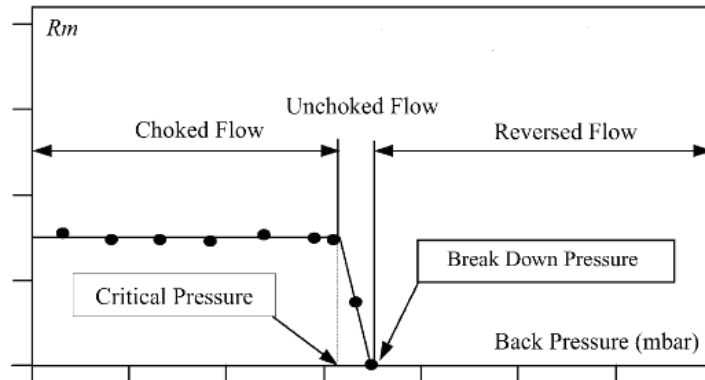


Figure 2: Ejector Performance Curve.

There are three zones of operation, distinguished by the critical pressure and the break down pressure. First is the choked flow zone, where back pressure is below the critical pressure. The secondary fluid shocks which causes a constant flow, maintained the same value of RM throughout the region. Second, the unchoked flow zone, where the back pressure is above the critical pressure and the secondary fluid doesn't shock. The secondary flow fall quickly as the back pressure increases. Finally, the reversed flow zone where the back pressure exceeds the break down pressure and reverse flow of secondary fluid occurs characterizing a malfunction region. Many past studies [KEENAN e NEUMANN (1942), CHUNNANOND e APHORNRATANA (2004), ESDU (1985) e APHORNRATANA e EAMES (1997)] show that, not only operating conditions, but ejector geometries were also found to affect the ejector performance.

To build the ejector's performance curve were performed several simulations keeping the inlet boundary conditions and varying the back pressure values. Table 2 present the back pressure values for each case.

Table 2: Back pressures for each case.

Case 1	Case 2	Case 3
30	30	30
33	35	35
35	40	40
37	45	45
38	47	46
39	48	47
40	49	48
41	50	49

42		50
		51
		52
		53

It was performed 29 simulations to analyze the performance curve for each case.

3 CFD MODEL SETUP

The simulations were performed in ANSYS Fluent 13.0 (ANSYS FLUENT theory guide, 2010), it was used density-based solver, which is more suitable for simulations of compressible flows and in all simulation the energy equation was solved.

The Steady-State transport equations are described below.

- Continuity Equation

$$\frac{\partial u_i}{\partial x_i} = 0 \quad (2)$$

- Momentum Equation

$$u_j \frac{\partial u_i}{\partial x_j} = -\frac{1}{\rho} \frac{\partial p}{\partial x_i} + \nu \frac{\partial^2 u_i}{\partial x_j \partial x_j} + \frac{\partial}{\partial x_j} \left(-\overline{u_i' u_j'} \right) \quad (3)$$

Where u_i is mean velocity component in x_i direction, ρ is the density, p is the mean pressure, ν is the kinematic viscosity, the overbar denotes time averaging, and the prime denotes fluctuating part.

3.1 Turbulence models

In this work were used three turbulence models, SST k- ω model, the SAS model and LES.

- SST k- ω Model

The SST k- ω by KARVINEN and AHLSTEDT (1994) is based on the boussinesq hypothesis. The Reynolds stresses, $-\overline{u_i' u_j'}$ are approximated with as follow:

$$-\overline{u_i' u_j'} = 2\nu_t S_{ij} - \frac{2}{3} k \delta_{ij}, \quad S_{ij} = \frac{1}{2} \left(\frac{\partial u_i}{\partial x_j} + \frac{\partial u_j}{\partial x_i} \right) \quad (4)$$

Where ν_t is the turbulent viscosity. This model blends the robust and accurate formulation of the k- ω model in the near-wall region with the free-stream independence of the k- ϵ model in the far field. Blend function are used to convert k- ϵ model into k- ω model. The

transport equations for this model are described below.

$$u_j \frac{\partial k}{\partial x_j} = \frac{\partial}{\partial x_j} \left[\left(\nu + \frac{\nu_t}{\sigma_k} \right) \frac{\partial k}{\partial x_j} \right] + \nu_t S^2 - \beta_\infty^* k \omega \quad (5)$$

$$u_j \frac{\partial \omega}{\partial x_j} = \frac{\partial}{\partial x_j} \left[\left(\nu + \frac{\nu_t}{\sigma_k} \right) \frac{\partial \omega}{\partial x_j} \right] + S^2 - \beta_i \omega^2 + D_\omega \quad (6)$$

Where $\beta_i = F_1 \beta_{i,1} + (1 - F_1) \beta_{i,2}$ where the turbulent viscosity is computed from $\mu_t = \frac{\rho k}{\omega} \frac{1}{\max \left[\frac{1}{a^*}, \frac{SF_2}{a_1 \omega} \right]}$. The quantity Ω is the mean rate-of-rotation, F_1 and F_2 are the

blending functions, and σ_k and σ_ω are the auxiliary functions. The term D_ω is the cross-diffusion term. The model constants are $a_1 = 0.31$, $\beta_\infty^* = 0.09$, $\beta_{i,1} = 0.075$, $\beta_{i,2} = 0.0828$, $\sigma_{k,1} = 1.176$, $\sigma_{\omega,1} = 2.0$, $\sigma_{k,2} = 1.0$ and $\sigma_{\omega,2} = 1.168$.

- SAS

It's is a URANS model developed originally by FROHLICH and TERZI, (2008), basically a transient RANS model. This model include a source term Q_{SAS} in the ω transport equation of SST k- ω , to minimize the effect to model the turbulence when this term is greater than zero. To calculate his value mesh and time step refinement have to be sufficient to capture turbulence effects. The Q_{SAS} equation is showed below.

$$Q_{SAS} = \max \left[\rho \xi_2 k S^2 \left(\frac{l}{l_{vk}} \right) - C \frac{2\rho k}{\sigma_\phi} \max \left(\frac{1}{\omega^2} \frac{\partial \omega}{\partial x_j} \frac{\partial \omega}{\partial x_j}, \frac{1}{k^2} \frac{\partial k}{\partial x_j} \frac{\partial k}{\partial x_j} \right), 0 \right] \quad (7)$$

Where, l is the modeled turbulence length scale and l_{vk} is the Von Karman length scale described below.

$$l = \frac{\sqrt{k}}{C_\mu^4 \omega} \quad (8)$$

$$l_{vk} = \frac{kS}{\frac{\partial^2 u_i}{\partial x_j \partial x_j} \frac{\partial^2 u_i}{\partial x_j \partial x_j}} \quad (9)$$

- LES

The LES concept is to resolve the large scales of turbulence and model the small scales using the grid refinement as a filter to decide which one will be resolved or modeled using a subgrid model, usually simpler than two equations RANS models. The original model was developed by SMAGORINSKY (1963) and uses the follow expression to evaluate the

turbulent viscosity.

$$\nu_t = (C_s \bar{\Delta})^2 |S|, \quad |S| = \sqrt{2S_{ij}S_{ij}} \quad (10)$$

An adaptation of original LES model is called dynamic LES, where C_s isn't a constant anymore. A second filter is used and the scales between the two filters are used like representative of small scales of turbulence being used to calculate C dynamically. This one was used in this work.

3.2 Computational Domain and Mesh

The experimental equipment was divided in four parts, primary nozzle, the mixing chamber, the constant-area throat and the subsonic diffuser, as shown in Figure 1.



The Table 3 shows the meshes used with different refinement levels and presents their statistics.

Table 3: Mesh Statistics.

Name	Elements	Nodes	Higher element volume (m³)	Smaller element volume (m³)
Mesh 1	971,733	950,633	$7.094 \cdot 10^{-9}$	$5.384 \cdot 10^{-13}$
Mesh 2	3,249,260	3,302,901	$1.779 \cdot 10^{-9}$	$7.854 \cdot 10^{-14}$
Mesh 3	3,086,656	3,115,870	$5.005 \cdot 10^{-10}$	$1.140 \cdot 10^{-13}$

SST $k-\omega$ and SAS simulations used the all three meshes, for LES simulation it was used only the mesh 3. Simulation with SST $k-\omega$ was made in steady-state condition whereas SAS and LES simulation were made in transient state with time step of 10^{-6} and 10^{-7} , respectively.

To calculate the characteristic time, it was used the smallest velocity between primary and secondary fluid from SST $k-\omega$ simulation results according to the following equation.

$$\text{Characteristic Time} = \frac{\text{Ejector Length}}{\text{primary Fluid Velocity}} \quad (11)$$

To ensure the development of the flow it was considered the simulation time as 3 times the characteristic time.

The computational time was around 48 hours for SST k- ω simulations, 60 hours for SAS simulations and 72 hours for LES simulations using 16 processing cores distributed by 2 machines with the follow configuration.

Table 4: Machine Configuration.

O.S:	Linux Red Hat
CPU:	Intel Xeon E5450
Speed (GHz):	3.0
CPU Count:	2
Network	Infiniband

4 RESULTS AND DISCUSSION

In this section the results will be presented. First, a grid resolution study with SST k- ω and SAS model will be discussed followed by a comparison between these models against LES model. The case used was case 2 (Table 1), this case is the most complicated to simulate because of the greater difference between the conditions of primary and secondary fluid.

4.1 Grid Study Resolution

Three different meshes refinements were used in this work. For SST k- ω and SAS all three meshes were used in simulations and for LES only mesh 3.

Figure 3 and Figure 4 show the comparison of pressure and Mach profile and Table 5 show the RM values calculated for simulations of each mesh with SST k- ω turbulence model, those values were compared with experimental data obtained from SRIVEERAKUL *et al* (2006).

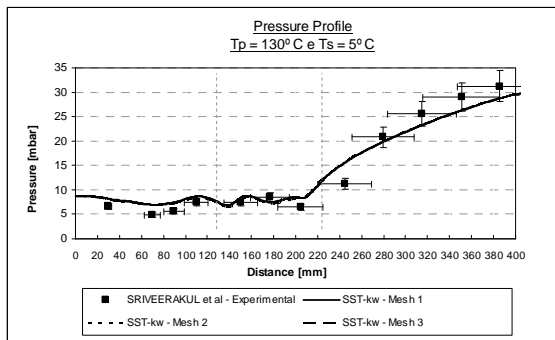


Figure 3: Pressure profile – SST k- ω .

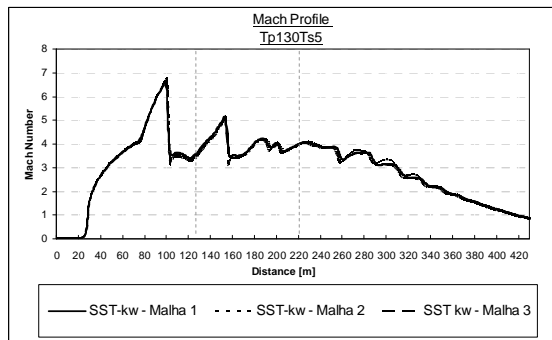


Figure 4: Mach profile – SST k- ω .

Table 5: Values for SST k- ω with 3 meshes (Case2).

	RM	%Error
Experimental	0.3087	0.00%
SST k-ω – mesh 1	0.2437	-21.06%
SST k-ω – mesh 2	0.2388	-22.64%
SST k-ω – mesh 3	0.2427	-21.38%

No difference between three meshes was observed. This behavior indicates the results independence against mesh for the SST k- ω model. For comparison with other models mesh 3 results were applied.

4.2 Comparison between models

Following, Figure 5 and Figure 6 show the comparison of pressure and Mach profile between SAS with all three meshes and SST k- ω with mesh 3. Table 6 show the RM values calculated for SAS compared with SST k- ω with mesh 3.

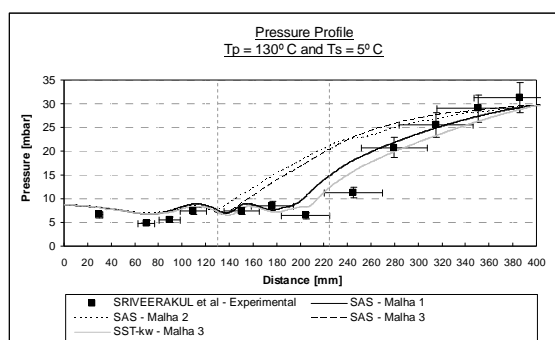


Figure 5: Pressure Profile – SAS.

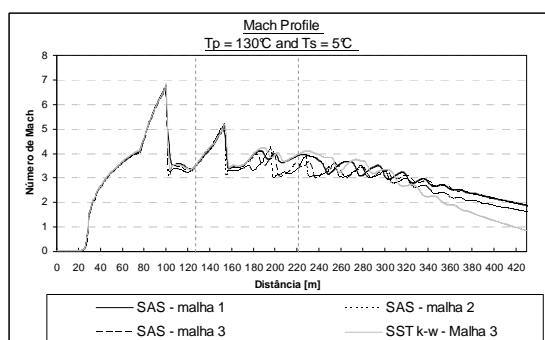


Figure 6: Mach profile – SAS.

Table 6:RM values for SAS with three meshes compared with SST k-w with mesh 3 (Case 2).

	RM	%Error
Experimental	0.3087	0.00%
SST k-ω –mesh 3	0.2437	-21.06%
SAS - mesh 1	0.2271	-26.43%
SAS - mesh 2	0.2281	-26.11%
SAS - mesh 3	0.2369	-23.26%

SAS model was more sensitive to mesh refinement than SST k- ω . The simulation with less mesh refinement (mesh 1) showed similar results compared to SST k- ω simulation. This behavior indicates that the mesh or time step refinement wasn't enough to compute QSAS and SAS model, reducing the SAS to SST k- ω .

Simulations with mesh 2 and 3 showed greater differences where SAS model showed an increase in pressure at a point above that seen in experimental data and a greater error with respect to experimental data when compared with SST k- ω .

Figure 7 shows the performance curve for case 2 using SST k- ω and SAS as turbulence models. The errors bars are 5%.

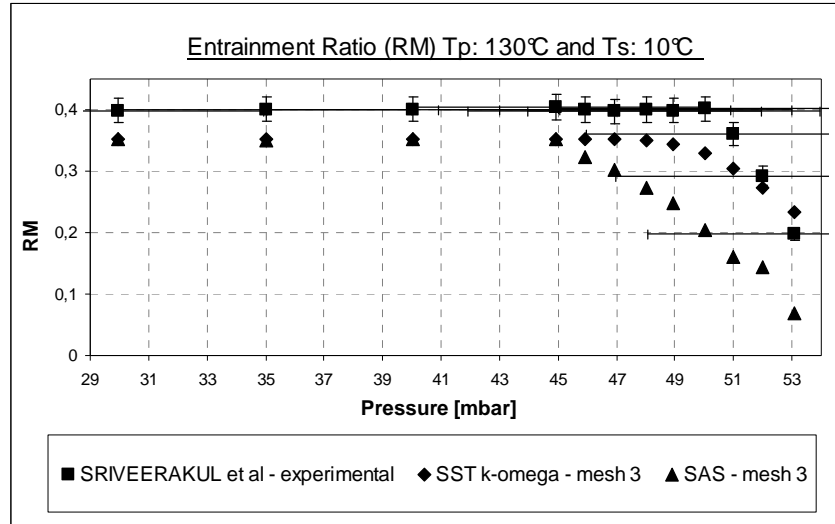


Figure 7: Performance Curve for SAS and SST k- ω with mesh 3.

Both SAS and SST k- ω anticipate critical point when compared with experimental data but SST k- ω nevertheless SST k- ω showed the best results. Table 7 shows the errors of those models related with experimental data.

Table 7: RM results for SAS and SST k- ω with mesh 3.

Case 2 Back Pressure (mbar)	RM			Errors	
	Exp.	SST k- ω	SAS	SST k- ω	SAS
30	0.3087	0.2437	0.2271	-21.06%	-26.43%
35	0.3110	0.2437	0.2269	-21.06%	-27.04%
40	0.3109	0.2437	0.2267	-21.06%	-27.08%
45	0.3096	0.2437	0.1755	-21.06%	-43.31%
46	0.3107	0.2293	0.1502	-26.20%	-51.66%
47	0.3107	0.2217	0.1198	-28.64%	-61.44%
48	0.3094	0.2053	0.0881	-33.65%	-71.52%
49	0.2284	0.1806	0.0543	-20.93%	-76.24%
50	0.0984	0.1496	0.0184	52.03%	-81.32%

SAS has the worst behavior for all points. The SAS worst error is close to 80% against SST k- ω with 50%. Both values occur for the same back pressure of 50 mbar.

Finally LES results were included in comparison with SAS and SST k- ω with mesh 3.

To compare LES model results with others mean variables (Mach and pressure) were calculated. Figure 8 and figure 9 show comparison of pressure and Mach profile including LES.

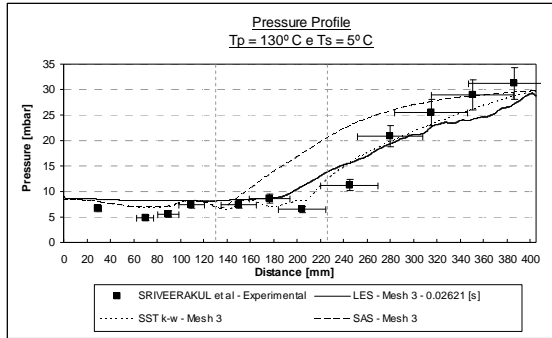


Figure 8: Pressure profile with LES.

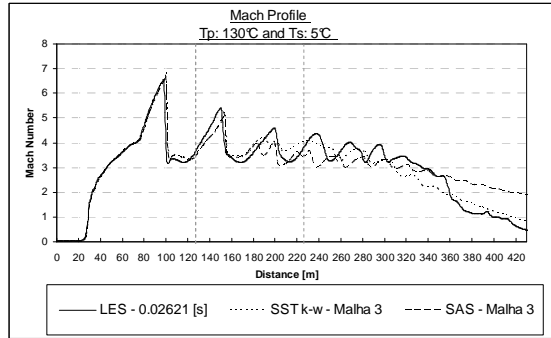


Figure 9: Mach Profile with LES.

LES model represents well experimental data although it has been compared mean value of variable but the SST k- ω still presents the smallest errors. The mach profile is correct with velocity peaks which decrease in amplitude over the ejector representing the dissipation of kinetic energy.

5 CONCLUSION

The ejector behavior was studied with three different turbulence models, SST k - ω , SAS and LES. SST k- ω was evaluated under steady state conditions and the others in transient condition. The main objective was to compare those models in capturing steam ejector supersonic flow characteristics analyzing pressure, Mach and RM values.

SST k- ω showed the best pressure profile agreement when compared with experimental data. The values of RM for SAS and SST k- ω models were close to 20%, when compared with experimental data. The understanding of this difference was not achieved yet as the CFD researcher still going.

SAS model was more sensitive to mesh refinement and simulation with less refined mesh showed results close to SST k- ω indicating that Q_{SAS} wasn't computed.

LES results showed a pressure profile similar to the experimental data. Temporal averages had influenced some points which presented a difference behavior, when compared to experimental data.

Some tests were performed in order to make the numerical results closer to experimental data but with no positive results. The reason of the numerical difference against experimental data is not clear yet, more research is need. Thus the SST k- ω model provides the best cost/benefit ratio for this simulation.

6 REFERENCES

MAN, H. C.; DUAN, J.; YUE, T.M.; Design and Characteristic Analysis of Supersonic Nozzles for high Gas Pressure Laser Cutting. *Journal of Materials Processing Technology*, 1997.

SCOTT, D.; AIDOUN, Z.; OUZANNE, M.; CFD Simulations of a Supersonic Ejector for Use in Refrigeration Application. *International Refrigeration and Air Conditioning Conference at Purdue*, 2008.

SRIVEERAKUL, T.; APHORNRATANA, S.; CHUNNANOND, K.; Performance prediction of steam ejector using computational fluid dynamics: Part 1. Validation of the CFD results. *International Journal of Thermal Sciences*, 2006.

ANSYS FLUENT Theory Guide, 2010.

ANSYS FLUENT USERS GUIDE, 2010.

J. H. KEENAN, E.P. NEUMANN, A simple air ejector, *ASME: Journal of Applied Mechanics* 64 (1942).

K. CHUNNANOND, S. APHORNRATANA, An Experimental investigation of a steam ejector. *Applied Thermal Engineering* 27 (2004).

ESDU, Ejector and jet pump, ESDU International Ltd, London, Data item 86030, 1985.

S. APHORNRATANA, I.W. EAMES, A small capacity steam-ejector refrigerator: experimental investigation of a system using with movable primary nozzle, *International Journal of Refrigeration* 20 (5) (1997).

J. SMAGORINSKY, General circulation experiments with the primitive equations: I. The basic experiment. *Mon. Weather Rev.* 91 (1963).

A. KARVINEN, H. AHLSTEDT, Comparison of turbulence models in case of jet cross flow using commercial CFD code. *Engineering Turbulence Modeling and Experiments* 6 (2005).

J. FROHLICH, D. VON TERZI, Hybrid LES/RANS methods for the simulation of turbulent flows. *Progress in Aerospace Sciences* 44 (2008) 349-377.